Importance of size-to-charge ratio in construction of stable and uniform nanoscale RNA/dendrimer complexes†

Xin-Cheng Shen,[a] Jiehua Zhou,[a] Xiaoxuan Liu,[a,b] Jiangyu Wu,[a,b] Fanqi Qu,[a] Zhi-Ling Zhang,[a] Dai-Wen Pang,*[a] Gilles Quéléver,[b] Cheng-Cai Zhang[c] and Ling Peng*[a,b]

Received 23rd July 2007, Accepted 18th September 2007
First published as an Advance Article on the web 2nd October 2007
DOI: 10.1039/b711242d

Formation of RNA/dendrimer complexes between various RNA molecules and PAMAM dendrimers was studied using atomic force microscopy. Our results demonstrate that effective construction of stable nanoscale and uniform RNA/dendrimer complexes depends critically on the size of the RNA molecule, the dendrimer generation and the charge ratio between the dendrimer and the RNA. Larger RNA molecules, higher generations of dendrimers and larger dendrimer-to-RNA charge ratios lead to the formation of stable, uniform nanoscale RNA/dendrimer complexes. These findings provide new insights in developing dendrimer systems for RNA delivery.

Introduction

RNA molecules are emerging as attractive therapeutic agents for the treatment of various diseases such as persistent cancers, neurodegenerative disorders and emerging global viral pandemic diseases.[1–5] However, the successful use of *in vitro*-synthesized RNA for therapeutic purposes depends critically on efficient means of RNA delivery. Very recently, we studied the use of polyamidoamine (PAMAM) dendrimers as self-assembling RNA delivery systems.[6] We demonstrated that PAMAM dendrimers and RNA molecules formed spontaneously self-assembled RNA/dendrimer complexes.[6–8] We also established that higher generation PAMAM dendrimers are efficient vectors for siRNA delivery.[6]

PAMAM dendrimers have been extensively studied as DNA delivery systems since the seminal studies by Szoka *et al.*[9] and Baker *et al.*[10] In dendrimer-mediated DNA delivery, the very first crucial issue on which efficient delivery depends is the formation of the DNA/dendrimer self-assembled complexes. The DNA/dendrimer complexes must be compact and small (around 100 nm) in order to ensure efficient cellular uptake by endocytosis and to protect DNA from enzymatic degradation. A similar situation may occur in the case of dendrimer-mediated RNA delivery, on which ongoing studies are still in a very preliminary stage.[6,11–14]

In our search for dendrimer systems for efficient delivery of various RNA molecules, we need to acquire more insight into the construction of stable uniform nanoscale RNA/dendrimer complexes, the very first crucial parameter. Although various aspects of the formation of nanometric DNA/dendrimer complexes have been described in the literature,[15–22] few efforts have been made so far with RNA/dendrimer complexes.[6–8,23,24] We therefore studied various RNA/dendrimer complexes using atomic force microscopy (AFM), a useful technique to investigate nanoscale complexes at high resolution. These studies, together with the results obtained by gel mobility shift assay and transmission electron microscopy (TEM), showed that the construction of uniform, stable nanoscale RNA/dendrimer complexes depends critically on the dendrimer-to-RNA charge ratio (the N/P ratio), the size of the RNA molecule and the dendrimer generation. We present herein the results of these studies. The RNA molecules used in our study are the small interfering RNA (siRNA, 21 bp), the *Candida* ribozyme (*Ca.*L-11, 368 nt, a self-splicing group I intron from the 26S rRNA of the opportunistic fungal pathogen *Candida albicans*),[25] and the poly(rU) (>2000 nt, an important component of the polyribonucleotide immunomodulators),[26] whereas the dendrimers are the PAMAM dendrimers developed in our laboratories, $\mathbf{G}_n$ (*n*: the dendrimer generation number), having a triethanolamine core and a generation number ranging from 1 to 7 (Scheme 1).[6,7] PAMAM dendrimers with a triethanolamine core are expected to have a more flexible structure because the branching units start away from the central amine with a distance of 10 successive bonds, whereas those of the commercial PAMAM dendrimers with an NH_3 or ethylenediamine core start at the central amine of the core.[27] Most importantly, we have recently demonstrated that the triethanolamine core PAMAM dendrimers efficiently inhibit the *Candida* ribozymes and deliver siRNA for gene silencing as well.[6,7]

Results and discussion

1. Synthesis

Synthesis of dendrimers $\mathbf{G}_n$ has already been described in our previous work.[6,7] We report herein the detailed synthesis of all the dendrimers $\mathbf{G}_n$ (Scheme 1) using an improved procedure for the preparation of the tri-nitrile derivative **1**, which is the starting material necessary for the building of the core for dendrimer growth. In our previous work, **1** was obtained in a

[a]*College of Chemistry and Molecular Sciences, Wuhan University, Wuhan, 430072, P. R. China*
[b]*Département de Chimie, CNRS UMR 6114, 163 avenue de Luminy, 13288, Marseille cedex 09, France. E-mail: ling.peng@univmed.fr; Fax: +33 491 82 93 01; Tel: +33 491 82 91 54*
[c]*Laboratoire de Chimie Bactérienne, CNRS UPR 9043, 31 chemin Joseph Aiguier, 13402, Marseille cedex 20, France*
† Electronic supplementary information (ESI) available: Tables S1 and S2. See DOI: 10.1039/b711242d

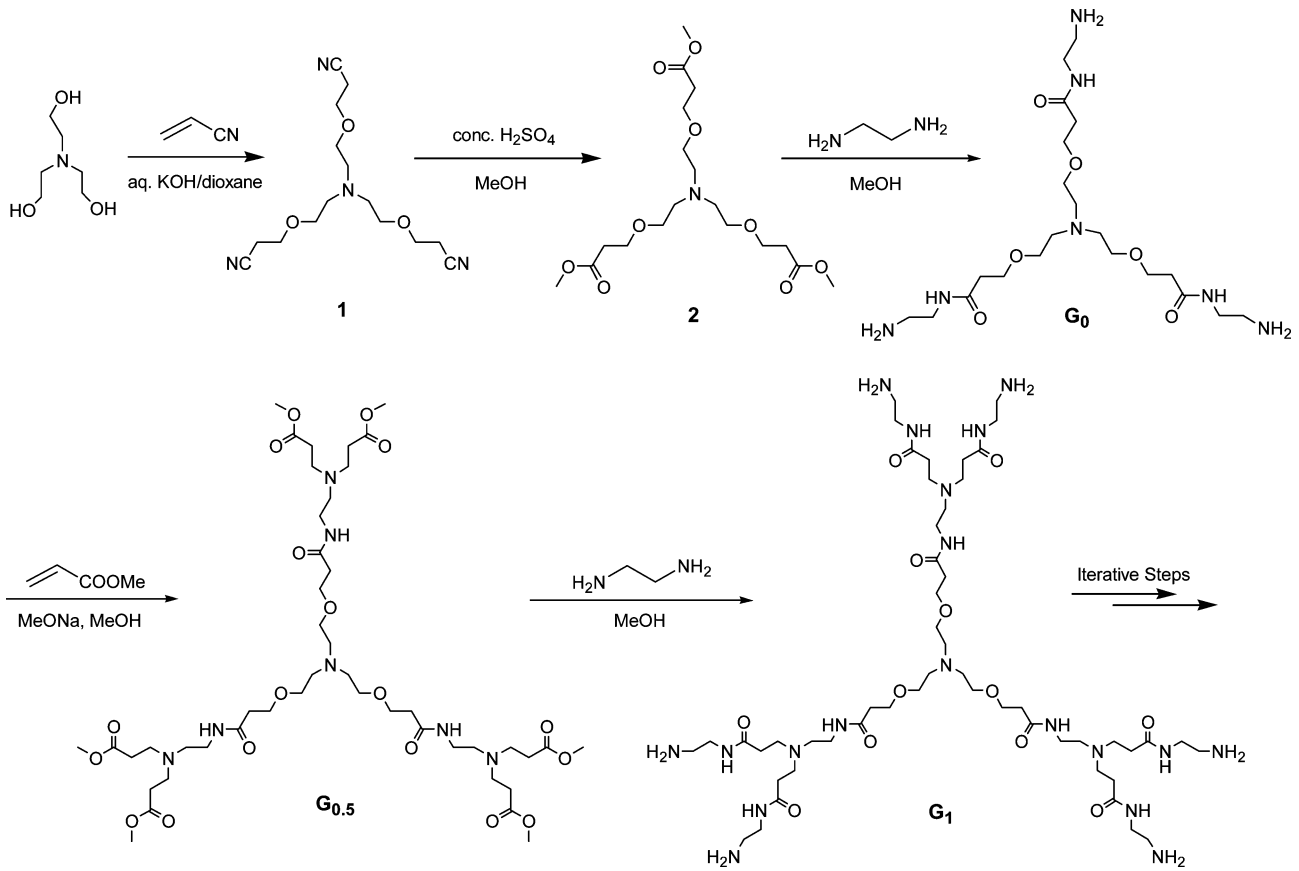

Scheme 1 Synthesis of PAMAM dendrimers with triethanolamine as the core.

yield of approximately 70% by Michael addition of acrylonitrile to triethanolamine, requiring a four-day reaction time. Now, we are able to isolate this tri-nitrile derivative **1** in an 81% yield while reducing significantly the reaction time to 16 hours at room temperature by employing the procedure described by Newkome *et al.*,[28] namely, using a catalytic amount of aqueous 3.6 M KOH in dioxane as solvent (Scheme 1).

From generations 1 to 7, the dendrimer growth was achieved using a conventional procedure involving a two-step iterative synthesis: (a) amidation of the terminal ester with ethylenediamine to generate the amine-terminated dendrimers, followed by (b) branching double alkylation of the terminal NH_2 groups with methyl acrylate, to generate the ester-terminated dendrimers.[6,7,27] The synthetic procedure for preparation of PAMAM dendrimers is well established and affords the corresponding products in nearly quantitative yields.

The dendrimer structures were further confirmed by FT-IR and NMR. The half-generation dendrimers with the ester-terminated groups display the characteristic IR peaks for a carbonyl group at 1730–1750 cm^{-1}. When the ester-terminated half-generation dendrimers were converted to the amine-terminated full-generation dendrimers, the methyl ester groups were transformed to the corresponding amide groups. This process could be monitored clearly by FT-IR, with the corresponding carbonyl signals being shifted from 1740 to 1650 cm^{-1}. The ^{1}H-NMR data corroborated well with the FT-IR data to confirm the structure of the dendrimers: the characteristic methyl ester peak, which appeared in all the NMR spectra of the ester-terminated dendrimers, was absent in the spectra of all the amine-terminated dendrimers.

The molecular weights of dendrimers from generations 1 to 3 could be determined by mass spectroscopy,[7,29] while those of dendrimers with higher generation could only be estimated by GPC analysis using commercial PAMAM dendrimers as references (Table 1). The obtained molecular weights were in good agreement with the theoretical values.

2. AFM study of free RNA molecules and free dendrimers

We first studied AFM images of free RNA molecules such as siRNA, ribozyme *Ca.*L-11 and poly(rU). None of these RNA molecules were observed on the unmodified free mica surface

Table 1 General information on dendrimers synthesized and used in the study

	Generation	End group number	MW[a]	MW[b]
G_1	1	6	1 177	1 177[c]
G_2	2	12	2 547	2 483
G_3	3	24	5 287	5 143
G_4	4	48	10 767	11 587
G_5	5	96	21 727	18 893
G_6	6	192	43 648	49 265
G_7	7	384	87 489	86 342

[a] From theoretical calculation. [b] From GPC estimation. [c] From ESI MS measurement.

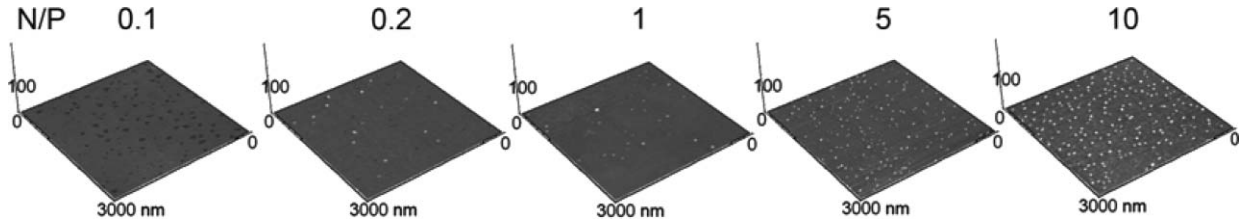

Fig. 1 AFM 3D images of the siRNA/$\mathbf{G_7}$ complexes at various N/P ratios from 0.1 to 10 at a final siRNA concentration of 0.0125 mg L^{-1}. From left to right, the N/P ratios are respectively 0.1, 0.2, 1, 5 and 10.

(data not shown). This is because both RNA and mica are negatively charged. Therefore, RNA molecules could not be stably immobilized on the bare mica due to the electrostatic repulsion, and were washed out by water during sample preparation.

We then studied PAMAM dendrimers. With dendrimer molecules $\mathbf{G_1}$ to $\mathbf{G_7}$, dendrimer aggregates could be observed at concentrations over 0.7 mg L^{-1}, while no obvious nanoparticles were detected for the pure dendrimers at lower concentrations (data not shown). This finding is consistent with the literature report:[30] dendrimers firstly form a film on the mica surface in order to maintain lower surface tension; then, with increasing concentration of dendrimers, excess dendrimer molecules aggregate on the surface of the dendrimer film to form the globular nanoparticles.

In order to avoid any interference which might result from free dendrimers or free RNA, we used dendrimers at low concentrations and an unmodified free mica surface for our AFM study of the RNA/dendrimer complexes.

3. AFM study of the RNA/dendrimer complexes

Charge ratio between RNA and dendrimer. Our previous results showed that the charge ratio N/P between the dendrimer $\mathbf{G_7}$ and siRNA is an important factor contributing to the formation of stable siRNA/dendrimer complexes and the efficient delivery of siRNA.[6] We therefore studied the siRNA/$\mathbf{G_7}$ complexes at various N/P charge ratios by AFM. At an N/P ratio of 0.1, AFM studies showed no nanoscale siRNA/$\mathbf{G_7}$ complexes but yielded only a perforated film. Very few small nanoscale and irregular spherical particles (D ~35 nm) were detected at N/P ratios of 0.2 and 1 (Fig. 1 and Table S1†), whereas significant numbers of uniform siRNA/$\mathbf{G_7}$ nanoparticles were clearly visible at N/P ratios of 5 and 10 (Fig. 1). At an N/P ratio of 10, the siRNA/$\mathbf{G_7}$ complexes were well-defined compact uniform spheroids (Fig. 1 and Fig. 2). The finding that the formation of stable siRNA/$\mathbf{G_7}$ complexes depends strongly on the dendrimer/RNA charge ratio is consistent with the results obtained by gel electrophoresis (Fig. 3c): the higher the charge ratio of dendrimer to RNA is, the more stable the RNA/dendrimer complexes are.[6–8,23]

Dendrimer generation. We also investigated the effects of the dendrimer generation on the effective construction of nanoscale RNA/dendrimer complexes. The AFM images of siRNA/dendrimer complexes are shown in Fig. 4 at an N/P ratio of 10 using dendrimers ranging from generations 1 to 7. As we can see in Fig. 4, few siRNA/dendrimer particles were observed with $\mathbf{G_1}$ to $\mathbf{G_3}$, while nanoscale particles started to appear with $\mathbf{G_4}$ and $\mathbf{G_5}$, and remarkably numerous siRNA/dendrimer nanoparticles were formed with $\mathbf{G_6}$ and $\mathbf{G_7}$. From generations $\mathbf{G_4}$ to $\mathbf{G_7}$, the siRNA/dendrimer nanoparticles became increasingly uniform, well-defined and compact (Fig. 4), which suggests that the dendrimers of higher generations are more apt to form nanoscale siRNA/dendrimer complexes. This is also in agreement with the results obtained by an RNA mobility shift assay (Fig. 3): no complete gel retardation was observed for the siRNA with $\mathbf{G_1}$ at an N/P ratio even up to 10, while $\mathbf{G_4}$ started to retard significantly the siRNA mobility at charge ratios N/P > 2.5, and $\mathbf{G_7}$ almost completely prevented the siRNA shift in the gels at a charge ratio of N/P = 2.5. The above data can also explain why $\mathbf{G_7}$ is an efficient siRNA delivery vector, since $\mathbf{G_7}$ forms much more stable nanoparticles with siRNA, which can effectively protect siRNA from enzymatic degradation and facilitate the endocytic uptake of the siRNA/dendrimer complexes by the cell.[6]

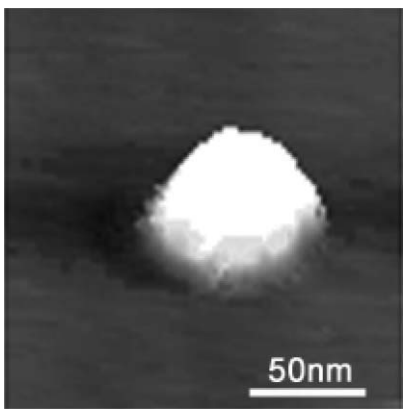

Fig. 2 AFM 3D image of a single spherical particle formed with siRNA/$\mathbf{G_7}$ complexes at an N/P ratio of 10 at a final siRNA concentration of 0.0125 mg L^{-1}.

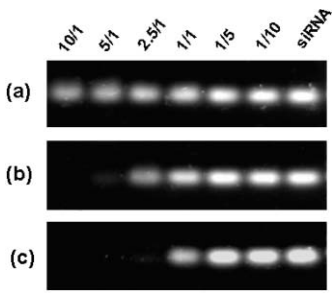

Fig. 3 Gel retardation of siRNA with different dendrimers (a) $\mathbf{G_1}$, (b) $\mathbf{G_4}$, and (c) $\mathbf{G_7}$ at various N/P ratios: 10 : 1, 5 : 1, 2.5 : 1, 1 : 1, 1 : 5 and 1 : 10 (from left to right).

RNA size. In order to study the influence of RNA size for the construction of the RNA/dendrimer complexes, we also studied

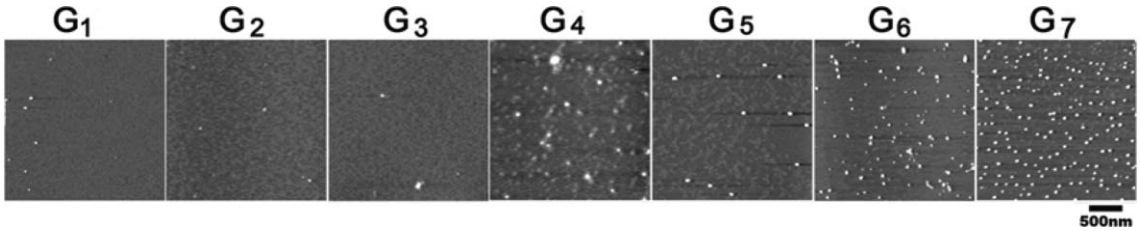

Fig. 4 AFM images of the siRNA/dendrimer complexes at an N/P ratio of 10 with dendrimers ranging from $\mathbf{G_1}$ to $\mathbf{G_7}$. The siRNA/dendrimer complexes were prepared at a final siRNA concentration of 0.0125 mg L^{-1}.

the RNA/$\mathbf{G_7}$ complexes using the *Candida* ribozyme *Ca.*L-11 and poly(rU). The *Candida* ribozyme *Ca.*L-11 has a length of 368 nt, while the poly(rU) is a larger RNA molecule with more than 2000 nt. With N/P ratios ranging from 0.1 to 10, both *Ca.*L-11 and poly(rU) formed increasingly uniform and compact nanoparticles with $\mathbf{G_7}$ (Fig. 5(a) and (b)). At the low N/P ratio of 0.1, $\mathbf{G_7}$ condensed the ribozyme *Ca.*L-11 into a few very small but collapsed nanoparticles (Fig. 5(a)). Interestingly, $\mathbf{G_7}$ formed well-defined globular nanoparticles with poly(rU), even at the low N/P ratio of 0.1 (Fig. 5(b)). These results indicate that strong cooperative effect and synergic interactions occurred between RNA and the dendrimers, and that these interactions intensified with the increasing size of the RNA molecule, resulting in the formation of more uniform, stable and compact RNA/$\mathbf{G_7}$ particles. Therefore, the formation of the nanoscale RNA/dendrimer complexes depends critically on both the N/P ratio and the size of the RNA molecules. With larger RNA molecules, the RNA molecules and dendrimers interweave more efficiently, leading to more cooperative interaction and therefore easier construction of nanoscale RNA/dendrimer complexes. The AFM data obtained with the *Candida* ribozyme agreed with the results obtained by the gel mobility shift assays,[7] and also confirmed our previous finding that RNA/dendrimers with a higher N/P ratio inhibit the ribozyme activity more efficiently.[7,8]

Further studies on dendrimer generation dependence using the ribozyme *Ca.*L-11 and poly(rU) yielded some intriguing results, different from those observed with siRNA (Fig. 4); both *Ca.*L-11 and poly(rU) formed spherical nanoparticles with dendrimers $\mathbf{G_1}$ to $\mathbf{G_7}$ at an N/P ratio of 10 (Fig. 6). For the lower generation dendrimers, the RNA molecules and the dendrimers were loosely condensed and less compacted, resulting in larger nanoparticles (Fig. 6, Table S2†). With increasing dendrimer

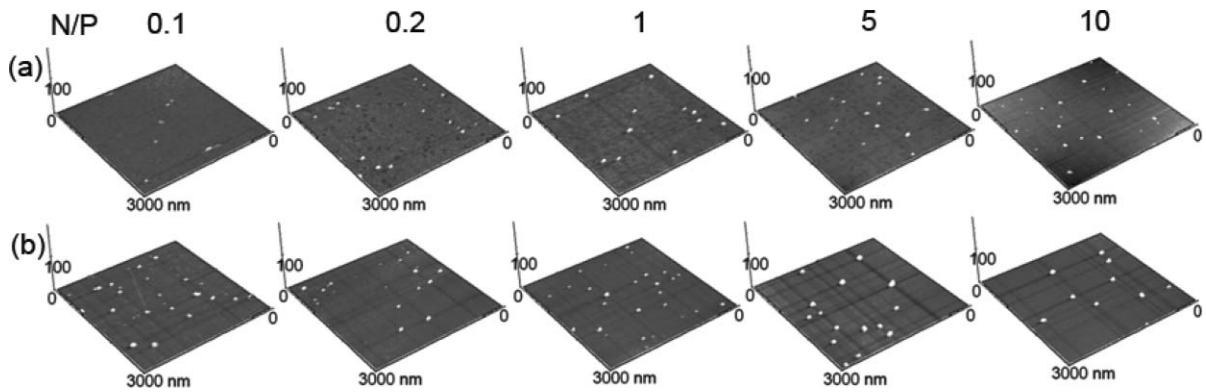

Fig. 5 AFM 3D images of the RNA/$\mathbf{G_7}$ complexes at various N/P ratios from 0.1 to 10 using (a) the *Candida* ribozyme *Ca.*L-11, and (b) poly(rU) at a final RNA concentration of 0.0125 mg L^{-1}. From left to right, the N/P ratios are respectively 0.1, 0.2, 1, 5 and 10.

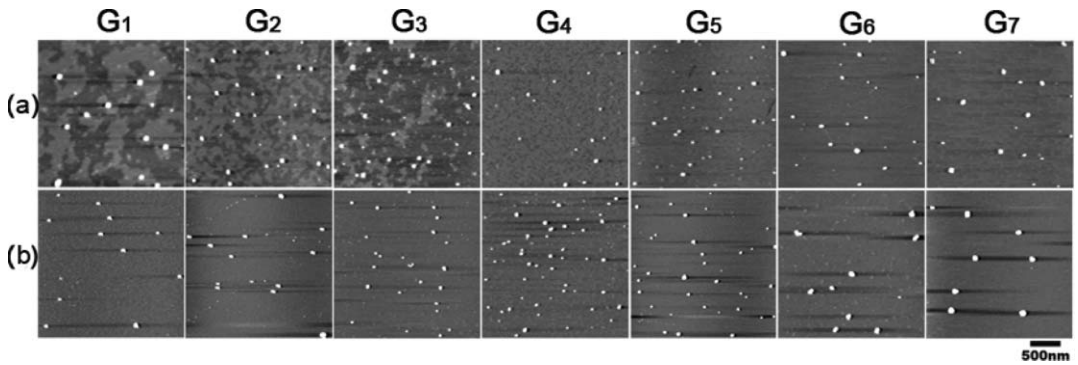

Fig. 6 AFM images of the RNA/dendrimer complexes at the N/P ratio of 10 with dendrimers ranging from $\mathbf{G_1}$ to $\mathbf{G_7}$ and the RNA molecules being (a) the *Candida* ribozyme, *Ca.*L-11, and (b) poly(rU). The RNA/dendrimer complexes were prepared at a final RNA concentration of 0.0125 mg L^{-1}.

generation, the RNA/dendrimer complexes were more densely compacted due to the cooperative effect and stronger interactions. This is further confirmed by the TEM on the RNA/dendrimer complexes (Fig. 7). As shown in Fig. 6, *Ca.*L-11 and $\mathbf{G_1}$ assembled only loosely in various sizes, while increasingly condensed and uniform nanoparticles were formed with $\mathbf{G_4}$ and $\mathbf{G_7}$. All the above results indicate also that both the RNA molecular sizes and the dendrimer generation are crucial for the construction of nanoscale RNA/dendrimer complexes. The higher the dendrimer generation is, the stronger the synergic interactions between dendrimers and RNA molecules will be, and consequently the more efficient the formation of the uniform and compact nanoscale RNA/dendrimer complexes will become. This finding is in agreement with the results obtained with DNA/dendrimer complexes: dendrimers of higher generations bind more tightly to longer DNA segments.[31]

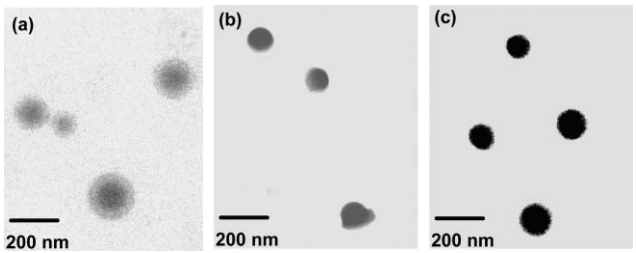

Fig. 7 TEM images of the *Ca.*L-11 RNA/dendrimer complexes: (a) RNA/$\mathbf{G_1}$, (b) RNA/$\mathbf{G_4}$, and (c) RNA/$\mathbf{G_7}$ complexes at an N/P ratio of 10.

Conclusions

The results presented in this study show that effective construction of uniform, stable nanoscale RNA/dendrimer complexes depends strongly on the charge ratio between dendrimer and RNA, the size of the RNA molecules and the generation of the dendrimers. The charge ratio is one of the most important factors which need to be taken into account in the construction of RNA/dendrimer particles. At the high N/P ratio of 10, $\mathbf{G_7}$ formed the most homogeneous spherical particles with various RNA molecules. With small RNA molecules such as siRNA (21 bp), only dendrimers of high generations can form stable, uniform and well-defined nanoscale siRNA/dendrimer particles. With larger RNA molecules such as the ribozyme *Ca.*L-11 (368 nt) and poly(rU) (>2000 nt), dendrimers from generations 1 to 7 readily form nanoparticles with RNA. This is the direct consequence of the strong electrostatic interaction occurring in the RNA/dendrimer complexes as well as of the cooperative and amplification effects exhibited by both RNA and dendrimer macromolecules. The results obtained in this work imply that higher generation dendrimers are required for better interaction and efficient delivery of the smaller siRNA molecules, which correlates well with our previous findings,[6] whereas lower generation dendrimers may be sufficient to provide strong interaction with[7,8] and efficient delivery of larger RNA molecules such as the *Candida* ribozyme and poly(rU). On the basis of these findings, the present work provides useful instruction and adds new perspectives to the development of efficient dendrimer systems for the delivery of various RNA molecules. We are working actively in this direction.

Experimental

Materials and methods

siRNA was purchased from Proligo LLS (Colorado, USA). The antisense sequence of siRNA is 5′-UCG AAG UAC UCA GCG UAA G dTdT-3′, and the sense sequence is 3′-dTdT AGC UUC AUG AGU CGC AUU C-5′. The *Candida* ribozyme *Ca.*L-11 was synthesized and purified as previously described.[7,8] Poly(rU) (>2000 nt) was purchased from Sigma. All other reagents and solvents of analytical grade were obtained from commercial sources and used without any further purification. Water (≥18.0 MΩ cm) was obtained from a Lab water Pro Plus system (Labconco, USA) and used freshly for the preparation of dendrimer and RNA solutions. All the tips, tubes and buffer solutions for RNA experiments were sterilized to prevent RNA from degradation by RNase digestion. AFM studies were performed on a Picoscan atomic force microscope (Molecular Imaging, USA) in MAC Mode (Magnetic AC Mode) using commercial Type II MAClevers probes (Molecular Imaging, USA) with a spring constant of 2.8 N m^{-1} and resonance frequency of 75 kHz. Measurements were carried out at 25 °C. Unless otherwise stated, data processing was limited to first- or second-order flattening using the Picoscan 4.19 SPM software program (Molecular Imaging, USA). The diameters of the particles in all the tables were obtained by performing Gaussian fitting on fifty measurements with Origin 7.0 at a confidence level of 0.95.

Dendrimer synthesis

Scheme 1 summarizes the synthesis of triethanolamine-derived PAMAM dendrimers from generation 1 to 7. To a solution of triester **2** in CH_3OH was added a large excess of ethylenediamine, and the reaction was stirred at room temperature for 1 day. The mixture was concentrated *in vacuo* to give the full-generation dendrimer $\mathbf{G_0}$. To a solution of $\mathbf{G_0}$ in CH_3OH was added methyl acrylate. The reaction mixture was stirred in dark at room temperature for 5 days. The reaction solution was concentrated *in vacuo* to afford the next half-generation dendrimers $\mathbf{G_{0.5}}$. To a solution of $\mathbf{G_{0.5}}$ in CH_3OH was added a large excess of ethylenediamine, and the reaction was stirred at room temperature for 1 day. The mixture was concentrated *in vacuo* to give the full-generation dendrimer $\mathbf{G_1}$. The iterative steps afford dendrimers from $\mathbf{G_2}$ to $\mathbf{G_7}$. Each generation of dendrimer was purified by precipitating the dendrimer from its MeOH solution with either ether (for amine-terminated dendrimers) or petroleum ether (for ester-terminated dendrimers). The precipitate was then dried *in vacuo*. This purification process was repeated more than three times for each dendrimer. Higher generation dendrimers were further subjected to dialysis.

$\mathbf{G_1}$. ^{1}H NMR (300 MHz, D_2O): δ 3.55 (t, 6H, J = 5.7 Hz), 3.42 (t, 6H, J = 5.4 Hz), 3.02–3.24 (m, 18H), 2.41–2.75 (m, 30H), 2.47 (t, 6H, J = 6.6 Hz), 2.34 (t, 6H, J = 5.7 Hz), 2.27 (t, 12H, J = 6.9 Hz); ^{13}C NMR (75 MHz, D_2O): δ 174.5, 173.3, 68.6, 67.1, 53.5, 51.8, 49.7, 49.4, 42.3, 42.2, 42.1, 40.4, 37.5, 36.8, 33.5; IR (cm^{-1}): ν 1643.0; MS (ESI): Calcd. for $C_{51}H_{105}N_{19}O_{12}$: 1176.8 $(M + H)^+$, 1198.8 $(M + Na)^+$, Found: 1176.7 $(M + H)^+$, 1198.7 $(M + Na)^+$.

$G_{1.5}$. According to the same procedure described for the synthesis of $G_{0.5}$, $G_{1.5}$ was obtained from G_1. ^{1}H NMR (300 MHz, $CDCl_3$): δ 3.67–3.71 (m, 6H), 3.60–3.66 (m, 42H), 3.21–3.33 (m, 18H), 2.77–2.84 (m, 12H), 2.68–2.77 (m, 30H), 2.49–2.63 (m, 18H), 2.32–2.44 (m, 42H); ^{13}C NMR (75 MHz, $CDCl_3$): δ 172.4, 172.3, 171.7, 68.0, 53.3, 52.6, 52.0, 50.4, 50.2, 49.7, 37.7, 36.5, 34.5, 33.3; IR (cm^{-1}): ν 1736.1, 1651.3; MS (ESI): Calcd. for $C_{99}H_{177}N_{19}O_{36}$: 1105.6 $(M + 2H)^{2+}$, Found: 1105.5 $(M + 2H)^{2+}$.

G_2. According to the same procedure described for the synthesis of G_1, G_2 was obtained from $G_{1.5}$. ^{1}H NMR (300 MHz, D_2O): δ 3.59 (m, 6H), 3.45 (m, 6H), 3.05–3.25 (m, 42H), 2.55–2.75 (m, 66H), 2.42–2.55 (m, 18H), 2.18–2.41 (m, 42H); ^{13}C NMR (150 MHz, D_2O): δ 175.1, 174.7, 173.9, 68.3, 66.7, 53.0, 51.3, 50.1, 49.1, 42.7, 41.8, 39.9, 36.8, 36.2, 32.9, 32.7; IR (cm^{-1}): ν 1642.5; MS (ESI): Calcd. for $C_{111}H_{225}N_{43}O_{24}$: 1273.9 $(M + 2H)^{2+}$, 849.6 $(M + 3H)^{3+}$, 637.5 $(M + 4H)^{4+}$, Found: 1274.1 $(M + 2H)^{2+}$, 849.6 $(M + 3H)^{3+}$, 637.5 $(M + 4H)^{4+}$.

$G_{2.5}$. According to the same procedure described for the synthesis of $G_{0.5}$, $G_{2.5}$ was obtained from G_2. ^{1}H NMR (300 MHz, $CDCl_3$): δ 3.60–3.73 (m, 84H), 3.20–3.35 (m, 42H), 2.77–2.88 (b, 12H), 2.68–2.77 (m, 78H), 2.49–2.67 (m, 42H), 2.33–2.46 (m, 90H); ^{13}C NMR (75 MHz, $CDCl_3$): δ 172.7, 172.0, 68.2, 53.5, 52.8, 52.3, 52.2, 50.4, 49.9, 37.9, 34.6, 33.5, 33.4; IR (cm^{-1}): ν 1735.9, 1647.6; MS (ESI): Calcd. for $C_{207}H_{369}N_{43}O_{72}$: 1538.2 $(M + 3H)^{3+}$, 1153.9 $(M + 4H)^{4+}$, Found: 1538.7 $(M + 3H)^{3+}$, 1154.2 $(M + 4H)^{4+}$.

G_3. According to the same procedure described for the synthesis of G_1, G_3 was obtained from $G_{2.5}$. ^{1}H NMR (300 MHz, D_2O): δ 3.58 (m, 6H), 3.45 (m, 6H), 3.02–3.25 (m, 90H), 2.53–2.80 (m, 114H), 2.40–2.53 (m, 42H), 2.18–2.40 (m, 90H); ^{13}C NMR (75 MHz, D_2O): δ 174.6, 174.2, 68.4, 67.0, 53.5, 51.8, 50.6, 49.6, 49.4, 43.2, 42.4, 40.4, 37.4, 33.5, 33.3; IR (cm^{-1}): ν 1645.5; MS (ESI): Calcd. for $C_{231}H_{465}N_{91}O_{48}$: 1331.9 $(M + 3H + Na)^{4+}$, 1065.7 $(M + 4H + Na)^{5+}$, Found: 1331.8 $(M + 3H + Na)^{4+}$, 1065.6 $(M + 4H + Na)^{5+}$.

$G_{3.5}$. According to the same procedure described for the synthesis of $G_{0.5}$, $G_{3.5}$ was obtained from G_3. ^{1}H NMR (300 MHz, $CDCl_3$): δ 3.62–3.76 (m, 156H), 3.16–3.38 (m, 90H), 2.62–2.98 (m, 186H), 2.48–2.62 (m, 90H), 2.24–2.48 (m, 186H); ^{13}C NMR (150 MHz, $CDCl_3$): δ 173.1, 172.4, 68.2, 53.0, 52.5, 52.3, 51.7, 50.2, 49.8, 49.3, 37.6, 37.2, 33.9, 32.8, 32.7; IR (cm^{-1}): ν 1733.8, 1646.1.

G_4. According to the same procedure described for the synthesis of G_1, G_4 was obtained from $G_{3.5}$. ^{1}H NMR (300 MHz, D_2O): δ 3.52–3.62 (m, 6H), 3.40–3.50 (m, 6H), 3.03–3.27 (m, 186H), 2.53–2.77 (m, 282H), 2.40–2.53 (m, 90H), 2.15–2.40 (m, 186H); ^{13}C NMR (150 MHz, D_2O): δ 175.1, 174.6, 68.2, 66.8, 53.0, 51.3, 50.1, 49.1, 44.4, 41.5, 40.4, 39.8, 36.8, 32.8, 32.7; IR (cm^{-1}): ν 1644.2.

$G_{4.5}$. According to the same procedure described for the synthesis of $G_{0.5}$, $G_{4.5}$ was obtained from G_4. ^{1}H NMR (300 MHz, $CDCl_3$): δ 3.60–3.76 (m, 300H), 3.20–3.38 (m, 186H), 2.70–2.84 (m, 378H), 2.51–2.62 (m, 186H), 2.29–2.48 (m, 378H); ^{13}C NMR (75 MHz, $CDCl_3$): δ 173.24, 173.17, 172.6, 53.1, 52.4, 51.9, 51.7, 51.5, 50.4, 50.0, 49.5, 37.4, 34.0, 32.9; IR (cm^{-1}): ν 1732.2, 1647.3.

G_5. According to the same procedure described for the synthesis of G_1, G_5 was obtained from $G_{4.5}$. ^{1}H NMR (300 MHz, D_2O): δ 3.03–3.14 (m, 378H), 2.58–2.70 (m, 378H), 2.38–2.56 (m, 378H), 2.15–2.30 (m, 378H); ^{13}C NMR (150 MHz, D_2O): δ 175.3, 174.8, 51.5, 50.2, 49.3, 41.5, 40.5, 39.9, 36.9, 33.0, 32.8; IR (cm^{-1}): ν 1643.7.

$G_{5.5}$. According to the same procedure described for the synthesis of $G_{0.5}$, $G_{5.5}$ was obtained from G_5. ^{1}H NMR (300 MHz, $CDCl_3$): δ 3.60–3.72 (m, 588H), 3.20–3.38 (m, 378H), 2.68–2.84 (m, 762H), 2.50–2.62 (m, 378H), 2.30–2.48 (m, 762H); ^{13}C NMR (75 MHz, $CDCl_3$): δ 173.3, 172.6, 53.2, 52.5, 51.9, 51.8, 50.4, 50.0, 49.5, 37.4, 34.0, 32.9; IR (cm^{-1}): ν 1732.5, 1645.8.

G_6. According to the same procedure described for the synthesis of G_1, G_6 was obtained from $G_{5.5}$. ^{1}H NMR (300 MHz, D_2O): δ 3.00–3.14 (m, 762H), 2.58–2.70 (m, 762H), 2.40–2.56 (m, 762H), 2.20–2.28 (m, 762H); ^{13}C NMR (150 MHz, D_2O): δ 175.2, 174.7, 51.4, 50.2, 49.3, 49.2, 42.2, 41.8, 39.9, 36.9, 32.9, 32.8, 32.7; IR (cm^{-1}): ν 1646.4.

$G_{6.5}$. According to the same procedure described for the synthesis of $G_{0.5}$, $G_{6.5}$ was obtained from G_6. ^{1}H NMR (300 MHz, $CDCl_3$): δ 3.58–3.80 (m, 1156H), 3.18–3.36 (m, 762H), 2.68–2.84 (m, 1530H), 2.50–2.64 (m, 762H), 2.28–2.48 (m, 1530H); ^{13}C NMR (75 MHz, $CDCl_3$): δ 173.3, 172.6, 53.2, 52.5, 51.9, 50.0, 49.5, 37.4, 34.0, 32.9; IR (cm^{-1}): ν 1735.1, 1647.1.

G_7. According to the same procedure described for the synthesis of G_1, G_7 was obtained from $G_{6.5}$. ^{1}H NMR (300 MHz, D_2O): δ 3.00–3.10 (m, 1530H), 2.57–2.72 (m, 1530H), 2.37–2.54 (m, 1530H), 2.14–2.28 (m, 1530H); ^{13}C NMR (150 MHz, D_2O): δ 175.3, 174.8, 51.5, 50.2, 49.3, 41.5, 40.5, 39.9, 36.9, 33.0, 32.8; IR (cm^{-1}): ν 1642.5.

GPC analysis

GPC experiments were performed on an Alliance Waters HPLC system equipped with Waters 515 HPLC pump, 2414 refractive index detector (Waters Corp.), 2487 dual wavelength UV absorbance detector (Waters Corp.), and Polymer Standards Service Novema NOA0830103E2 (300 × 8 mm, 10 μm) columns. An Elite guard column was used to protect the column. The column temperature was maintained at 30 °C. The temperature of the refractive index detector was maintained as well at 30 °C. The isocratic mobile phase was 0.3 M formic acid and 0.1 M sodium chloride, pH 1.90, at a flow rate of 1.0 mL min^{-1}. Sample concentration was 1.0 mg mL^{-1} with an injection volume of 20 μL. The molecular weight of the dendrimer was determined with Empower Pro software (Waters Corp.) using commercial ethylenediamine-core PAMAM dendrimers from generation 1 to 7 (Aldrich) as references.[32]

AFM imaging of dendrimers

The dendrimer solutions were prepared to an appropriate concentration. The dendrimer concentrations were 8.6×10^{-4}, 8.6×10^{-3}, 8.6×10^{-2}, 7.0×10^{-1} and 7.0 mg L^{-1} for dendrimers from G_1 to G_7. 5 μL of each solution were deposited on freshly cleaved mica and kept for 5 minutes, allowing the dendrimer to adsorb on the mica surface. The adsorption process was carried out under a humid atmosphere in order to avoid the sample being dried. The mica surface was then rinsed with water, dried under a nitrogen flow, and subjected immediately to AFM study.

AFM imaging of RNA molecules

The AFM studies of various RNA molecules on free mica were undertaken under the same conditions as those described above for dendrimers. The final concentration of RNA solutions was 0.0125 mg L^{-1}.

AFM imaging of RNA/dendrimer complexes

In the AFM experiments, the concentration of the RNA solution was 0.025 mg L^{-1} for all the RNA molecules, while those of dendrimers $\mathbf{G_1}$ to $\mathbf{G_7}$ were 1.7×10^{-3}, 3.4×10^{-2}, 1.7×10^{-2}, 8.6×10^{-2} and 1.7×10^{-1} mg L^{-1}. 5 μL of the RNA solution (0.025 mg L^{-1}) was mixed with 5 μL of the dendrimer solution, and the mixed solution was kept at 25 °C for 30 minutes. Then, 5 μL of the obtained solution was deposited on freshly cleaved mica and kept under a humid atmosphere for 5 minutes, allowing the RNA/dendrimer complexes to adsorb on to the mica surface. The mica surface was then rinsed with water, dried under a nitrogen flow and subjected to AFM study immediately. The size of the RNA/dendrimer complexes was measured by cross-section analysis using the Picoscan 4.19 SPM software program (Molecular Imaging, USA).

Agarose gel analysis of RNA/dendrimer complexes

The dendrimers were prepared to an appropriate concentration in 50 mM Tris-HCl buffer (pH 7.6), mixed with the corresponding siRNA or ribozyme RNA solution at various N/P ratios (= [total end amines in dendrimer]/[phosphates in RNA]) and then incubated at 37 °C for 30 minutes. The final concentration of RNA was adjusted to 25 mg L^{-1} (100 ng per well). RNA/dendrimer complexes were analyzed by electrophoretic mobility shift assays in 1.2% agarose gel in standard TAE buffer. The RNA bands were stained by ethidium bromide and then detected by a Kodak 290 digital camera.[33]

Transmission electron microscopic study on the RNA/dendrimer complexes

TEM studies were performed with a JEM-1230 transmission electron microscope. 10 μL of an RNA solution (5 mg L^{-1} RNA) were mixed with 10 μL of a dendrimer solution (34 mg L^{-1}) in 50 mM Tris-HCl buffer and kept at room temperature for 30 minutes, allowing the formation and equilibration of the RNA/dendrimer complexes. 4 μL of the obtained mixture was dropped on to a standard carbon-coated copper TEM grid, and allowed to dry in air (1 h at 30 °C, ambient pressure). The grid was then stained with uranyl acetate (2% in water, pH 4.5) for 3 minutes, air-dried for 20 minutes, and TEM imaging was performed immediately.

Acknowledgements

This research was funded by the Ministry of Science and Technology of China (No. 2003CB114400), the National Natural Science Foundation of China (Nos. 20572081, 20025311, 30370404 and 30570490), Wuhan University, CNRS, AFM (Nos. 13074 and 10793) and PPF CNP2 (No. 20042462). The authors thank Prof. Yi Zhang for providing the genomic DNA of *C. albicans* and Ming-Xi Zhang for his help in processing all the figures. XCS, JHZ and XXL contributed equally to this work.

References and notes

1 B. A. Sullenger and E. Gilboa, *Nature*, 2002, **418**, 252.
2 G. J. Hannon and J. J. Rossi, *Nature*, 2004, **431**, 371; D. H. Kim and J. J. Rossi, *Nat. Rev. Genet.*, 2007, **8**, 173; A. de Fougerolles, H.-P. Vornlocher, J. Maraganore and J. Lieberman, *Nat. Rev. Drug Discovery*, 2007, **6**, 443.
3 L. Wohlbold, H. van der Kuip, C. Miething, H.-P. Vornlocher, C. Knabbe, J. Duyster and W. E. Aulitzky, *Blood*, 2003, **102**, 2236.
4 S. Q. Harper, P. D. Staber, X. H. He, S. L. Eliason, I. H. Martins, Q. W. Mao, L. Yang, R. M. Kotin, H. L. Paulson and B. L. Davidson, *Proc. Natl. Acad. Sci. U. S. A.*, 2005, **102**, 5820.
5 B.-J. Li, Q. Q. Tang, D. Cheng, C. Qin, F. Y. Xie, Q. Wei, J. Xu, Y. J. Liu, B.-J. Zheng, M. C. Woodle, N. S. Zhong and P. Y. Lu, *Nat. Med.*, 2005, **11**, 944.
6 J. H. Zhou, J. Y. Wu, N. Hafdi, J.-P. Behr, P. Erbacher and L. Peng, *Chem. Commun.*, 2006, 2362.
7 J. Y. Wu, J. H. Zhou, F. Q. Qu, P. H. Bao, Y. Zhang and L. Peng, *Chem. Commun.*, 2005, 313.
8 J. H. Zhou, J. Y. Wu, X. X. Liu, F. Q. Qu, M. Xiao, Y. Zhang, L. Charles, C.-C. Zhang and L. Peng, *Org. Biomol. Chem.*, 2006, **4**, 581.
9 J. Haensler and F. C. Szoka, Jr., *Bioconjugate Chem.*, 1993, **4**, 372; M. X. Tang, C. T. Redemann and F. C. Szoka, Jr., *Bioconjugate Chem.*, 1996, **7**, 703.
10 J. F. Kukowska-Latallo, A. U. Bielinska, J. Johnson, R. Spindler, D. A. Tomalia and J. R. Baker, Jr, *Proc. Natl. Acad. Sci. U. S. A.*, 1996, **93**, 4897; A. U. Bielinska, J. F. Kukowska-Latallo and J. R. Baker, Jr, *Biochim. Biophys. Acta*, 1997, **1353**, 180.
11 H. Kang, R. DeLong, M. H. Fisher and R. L. Juliano, *Pharm. Res.*, 2005, **22**, 2099; A. J. Hollins, M. Benboubetra, Y. Omidi, B. H. Zinselmeyer, A. G. Schatzlein, I. F. Uchegbu and S. Akhtar, *Pharm. Res.*, 2004, **21**, 458.
12 T. Tsutsumi, F. Hirayama, K. Uekama and H. Arima, *J. Controlled Release*, 2007, **119**, 349; T. Tsutsumi, H. Arima, F. Hirayama and K. Uekama, *J. Inclusion Phenom. Macrocyclic Chem.*, 2006, **56**, 81.
13 A. J. Hollins, Y. Omidi, I. F. Benter and S. Akhtar, *J. Drug Targeting*, 2007, **15**, 83; H. Baigude, J. McCarroll, C.-S. Yang, P. M. Swain and T. M. Rana, *Chem. Biol.*, 2007, **2**, 237.
14 R. Juliano, H. Kang, A. Astriab-Fisher, P. Herdewijn, P. Chaltin and A. Van Aerschot, *World Pat.* WO 113 571, 2005; D. A. Tomalia and B. H. Huang, *World Pat.* WO 088 958, 2006.
15 C. C. Lee, J. A. MacKay, J. M. J. Fréchet and F. C. Szoka, *Nat. Biotechnol.*, 2005, **23**, 1517; D. A. Tomalia, L. A. Reyna and S. Svenson, *Biochem. Soc. Trans.*, 2007, **35**, 61.
16 M. Guillot-Nieckowski, S. Eisler and F. Diederich, *New J. Chem.*, 2007, **31**, 1111; C. Dufès, I. F. Uchegbu and A. G. Schtäzlein, *Adv. Drug Delivery Rev.*, 2005, **57**, 2177.
17 M. X. Tang and F. C. Szoka, *Gene Ther.*, 1997, **4**, 823.
18 T. Kim, H. J. Seo, J. S. Choi, H.-S. Jang, J. Baek, K. Kim and J.-S. Park, *Biomacromolecules*, 2004, **5**, 2487; J.-B. Kim, J. S. Choi, K. Nam, M. Lee, J.-S. Park and J.-K. Lee, *J. Controlled Release*, 2006, **114**, 110; J. S. Choi, K. S. Ko, J.-S. Park, Y.-H. Kim, S. W. Kim and M. Lee, *Int. J. Pharm.*, 2006, **320**, 171.
19 D. Joester, M. Losson, R. Pugin, H. Heinzelmann, E. Walter, H. P. Merkle and F. Diederich, *Angew. Chem., Int. Ed.*, 2003, **42**, 1486; M. A. Kostiainen, J. G. Hardy and D. K. Smith, *Angew. Chem., Int. Ed.*, 2005, **44**, 2556.
20 K. C. Wood, S. R. Little, R. Langer and P. T. Hammond, *Angew. Chem., Int. Ed.*, 2005, **44**, 6704.
21 M.-L. Örberg, K. Schillén and T. Nylander, *Biomacromolecules*, 2007, **8**, 1557.
22 M. Guillot-Nieckowski, D. Joester, M. Stöhr, M. Losson, M. Adrian, B. Wagner, M. Kansy, H. Heinzelmann, R. Pugin, F. Diederich and J.-L. Gallani, *Langmuir*, 2007, **23**, 737.
23 J.-H. S. Kuo and Y. L. Lin, *J. Biotechnol.*, 2007, **129**, 383.
24 W. Wang, Z. P. Guo, Y. Chen, T. Liu and L. Jiang, *Chem. Biol. Drug Des.*, 2006, **68**, 314; H. Zhao, J. R. Li, F. Xi and L. Jiang, *FEBS Lett.*, 2004, **563**, 241.
25 Y. Zhang and M. J. Leibowitz, *Nucleic Acids Res.*, 2001, **29**, 2644.
26 W. Braun and M. Nakano, *Science*, 1967, **157**, 819; A. G. Johnson, *Clin. Microbiol. Rev.*, 1994, **7**, 277.

27 D. A. Tomalia, H. Baker, J. Dewald, M. Hall, G. Kallos, S. Martin, J. Roeck, J. Ryder and P. Smith, *Polym. J.*, 1985, **17**, 117; D. A. Tomalia, A. M. Naylor and W. A. Goddard, III, *Angew. Chem., Int. Ed. Engl.*, 1990, **29**, 138.
28 G. R. Newkome and X. F. Lin, *Macromolecules*, 1991, **24**, 1443; P. Basu, V. N. Nemykin and R. S. Sengar, *Inorg. Chem.*, 2003, **42**, 7489.
29 R. Giordanengo, M. Mazarin, J. Wu, L. Peng and L. Charles, *Int. J. Mass Spectrom.*, 2007, **266**, 62.
30 J. Li, L. T. Piehler, D. Qin, J. R. Baker, Jr. and D. A. Tomalia, *Langmuir*, 2000, **16**, 5613.
31 W. Chen, N. J. Turro and D. A. Tomalia, *Langmuir*, 2000, **16**, 15.
32 Because of the special architecture of the dendrimer molecules, we used well-defined commercial PAMAM dendrimers rather than other polymer standards as references for molecular weight calculation of our dendrimers. Under the GPC conditions we used, the peak of the dendrimer molecular weight agrees well with the theoretical value, although aggregation was observed for higher generation dendrimers.
33 We note here that we were not able to study the poly(rU)/dendrimer complexes by gel mobility shift assays because poly(rU) could not be efficiently stained by ethidium bromide.